Temperature Influence on the Morphology and Roughness of Silver Deposit Formed by Cementation

by **Grzegorz D. Sulka*** and **Marian Jaskuła**

Department of Physical Chemistry, Faculty of Chemistry, Jagiellonian University, Ingardena 3, PL-30-060 Krakow (phone: +48-12-663-2266; fax: +48-12-634-0515; e-mail: sulka@chemia.uj.edu.pl)

The morphology and surface roughness of silver deposits formed by cementation in 0.5M H_2SO_4 solution containing 0.5M $CuSO_4$ was investigated at various temperatures. The influence of O_2 on the morphology of deposited Ag on the Cu surface was studied in solutions containing 20 or 100 mg/dm^3 initial Ag^+. Surface-height-distribution diagrams were calculated from scanning-electron-microscopic (SEM) images. For the lower Ag^+ concentration, the formation of granular deposits occurred in the presence of O_2. In contrast, under anaerobic conditions, rather flat deposits with tiny Ag crystals were observed. For the higher Ag^+ concentration, the presence of O_2 did not significantly affect the morphology of the Ag deposit, but increasing temperature resulted in more-compact and denser dendrites. Differences in the Ag-deposit morphology and surface roughness were attributed to a different mechanism in the absence of O_2. Under anaerobic conditions, a competitive reaction between Ag^+ and Cu^+ occurs in bulk solution, which consumes additional Ag^+ ions. The SEM images and, especially, distribution diagrams of the surface height provided useful information on the formation and expansion of anodic sites on the Cu surface at various temperatures.

Introduction. – Electrochemical cementation is a heterogeneous redox reaction involving reduction of more-electropositive metal ions at cathodic sites and dissolution of a less-noble metal at anodic sites. The cementation process leads to the deposition of noble metal on a reaction surface and, consequently, to a significant reduction of the concentration of noble-metal ions in solution. Obviously, as a result of the anodic half-cell reaction involving dissolution of less-noble metal, the concentration of the sacrificial metal ion increases in solution. However, both cathodic and anodic sites are short-circuited and located on the same surface of a sacrificial solid metal.

Contrary to the complicated nature of the process, the application of cementation to various industrial processes is well-known and widely recognized. Applications are situated in the fields of traditional hydrometallurgy [1–6], electroplating and electrowinning [7–10], as well as purification of electrolytes [11–14], and waste treatment [15–19]. Recently, the scientific focus has been directed onto production of alloyed powders [20] and growth of nanowires on metal plates by cementation [21]. Cementation has been also applied as a very effective method for defect testing in PVD coatings [22]. The motor industry and, especially, new power-sources industry shifts traditional applications of the cementation process to a new region connected with the preparation of leady oxide for lead–acid batteries [23] and the manufacture of platinum-layer-modified Al electrodes by cementation [24]. Such a modified electrode can be applied for electro-oxidation of MeOH in fuel cells used in future electric-powered vehicles.

These modern applications of the cementation process often require a specific and well-defined morphology of the reaction product, *e.g.*, leady oxide powders [23] or Ag wires [21]. Therefore, the investigation of the morphology and roughness of deposit formed during cementation is very important.

Recently, we have reported that the Ag^+/Cu cementation reaction at the initial stage of the process follows first-order kinetics [25][26]. At the latter stage of the process, the kinetics and mechanism of cementation depend on the presence of O_2 in the system. Under O_2-free conditions, the following competitive reaction to cementation can proceed in bulk solution:

$$Ag^+ + Cu^+ \rightarrow Cu^{2+} + Ag^0_{colloid} \quad (1)$$

However, the presence of O_2 does not significantly affect the morphology of Ag deposits formed at 25° [26][27].

The present paper is focused on the temperature influence on the morphology and, especially, the surface roughness of Ag deposits formed by cementation conducted in the presence or absence of O_2, and the results are discussed in terms of change in mechanism.

Experimental. – All chemicals purchased were of anal. grade, and four-times-distilled H_2O was used to prepare all solns. Experiments were conducted in a rotating cylinder system described previously [25]. The rotating steel cylinder had a diameter of 1.175 cm, and a length of 7.450 cm. Before each run, the cylinder was carefully pre-treated, which included immersion in HNO_3/H_2O 1:1 (*v*/*v*), thorough rinsing with H_2O, and degreasing with MeOH. Then, the steel cylinder was covered with a fresh 24-μm-thick layer of Cu by electrolysis at a constant current of 36.4 mA/cm^2 for 30 min at 20° in an electrolyte containing 0.5M H_2SO_4 and 0.5M $CuSO_4$. The deposited Cu layer was electropolished at a constant current of 72.7 mA/cm^2 for 40 s at 20° in H_3PO_4/H_2O 3:1 (*v*/*v*), and then chemically polished for 1 min in 0.5M aq. H_2SO_4 soln. at 20°. After polishment, the cylinder was rinsed, air-dried, and used for cementation.

The electrolyte used for cementation tests was made from 0.5M H_2SO_4 and 0.5M $CuSO_4$ in the presence of 20 or 100 mg/dm^3 of Ag^+ ions (Ag_2SO_4). The initial concentration of Ag^+ in the studied soln. was determined before the experiment by atomic-absorption spectroscopy (AAS). The electrolyte used in each experiment had a volume of 200 ml, and was stirred at 500 r.p.m. The cementation tests were carried out in a temp. range of 15–55°. Before each run, the electrolyte in the cell was purged by bubbling with high-purity Ar gas or high-purity O_2 for 20 min. The O_2-free or O_2-sat. atmospheres were maintained over the solns. throughout the whole process by passing Ar or O_2. The duration of each experiment was 60 min. After each run, the Cu layer with cemented Ag was rinsed carefully, dried, cut, and separated from the cylinder. Two samples of the Cu sheet with cemented Ag were taken, dissolved in hot HNO_3/H_2O 1:1 (*v*/*v*), and analyzed for Ag content by AAS. The surface area of each sample taken for AAS analysis was *ca.* 3.5 cm^2. For each cementation test, the surface of two samples of the Ag-cemented Cu sheet was observed with a *Hitachi S-4700* scanning electron microscope (SEM). SEM Images were analyzed with the scanning probe image processor *WSxM 3.0 Beta* [28].

Results and Discussion. – The temperature influence on the morphology and roughness of Ag deposits formed in the cementation process was investigated both in O_2-free and O_2-saturated solutions at two initial concentrations of Ag^+. *Fig. 1* shows the SEM top-view images of the Cu surface with cemented Ag, together with their surface-height-distribution diagrams, for various temperatures under O_2-free conditions at an initial concentration of 20 mg/dm^3 Ag^+. The analyzed surface area of the samples was *ca.* 500 μm^2. During the cementation process, formation of cathodic and anodic

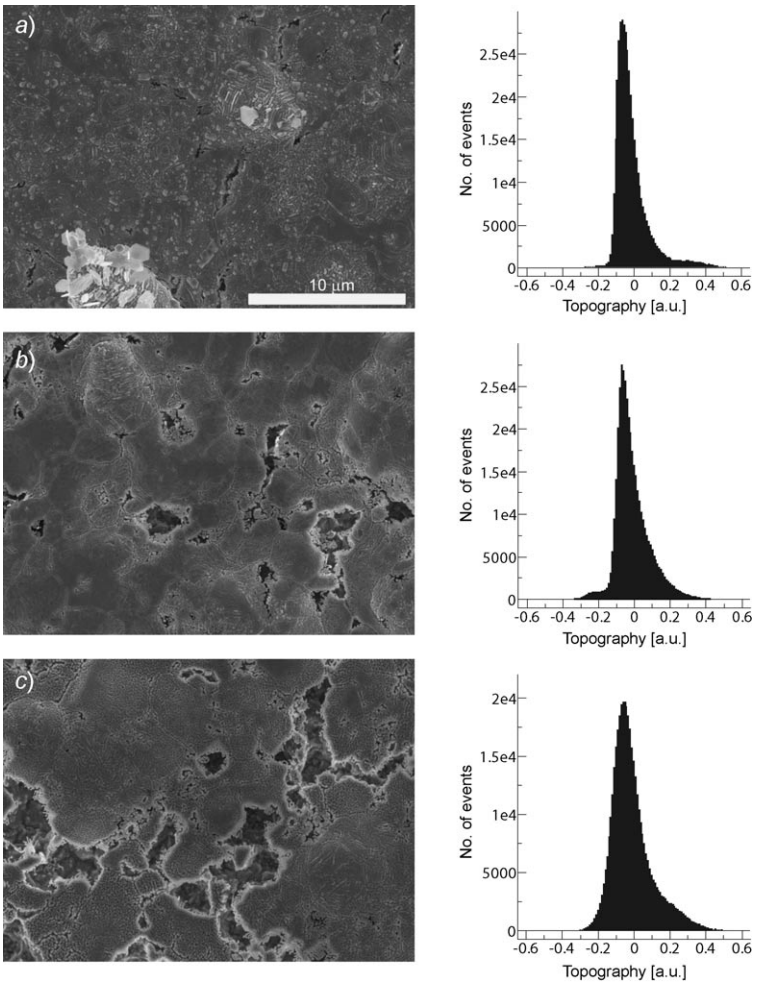

Fig. 1. *SEM Top-view images and surface-height-distribution diagrams for an O_2-free solution containing 20 mg/dm^3 Ag^+ at* a) *15°,* b) *35°, and* c) *55°*. Analyzed surface area: ca. 500 µm^2. For details, see *Experimental.*

sites occurs at the same time. The cathodic sites are formed on parts of the Cu surface, where a deposition of Ag occurs. The deposition of Ag proceeds preferentially on a protrusion existing on the Cu surface. As a result of the reaction progress, a dendrite grew on such a protrusion (*Fig. 1*,*a*).

As expected, with increasing temperature, the cementation rate increased rapidly (*Table 1*), and germs of cathodic sites were regularly spread over the reaction surface. At the same time, increasing temperature also promoted the progress of the reaction in bulk solution according to *Eqn. 1*. However, this reaction does not start below a temperature of *ca.* 25° [25]. As a result, no visible dendrite was observed in the SEM images at temperatures higher than 15° (*Figs. 1*,*b* and *1*,*c*). At higher temperatures, the catho-

dic sites were smoothly covered with Ag deposit, and a flattening effect of the surface roughness occurred. Anodic sites appeared on the Cu surface in forms of cracks, cavities, and holes visible in SEM images as dark spots. From the images presented in *Fig. 1*, it is clearly visible that, with increasing temperature, the surface area of the anodic sites increased rapidly due to an increasing rate of cementation (*Table 1*).

Table 1. *Reduced Average Rate Constants* ($k' = k/\omega^{0.701} \times 10^{-4}$; in cm/s) *Determined by Atomic-Absorption Spectroscopy for the Initial Cementation Period* (first few minutes) *as a Function of Temperature under Aerobic or Anaerobic Conditions.* $[Ag^+]_0$ corresponds to the initial solution concentration of silver, *n* is the number of independent cementation experiments. For details, see *Experimental*.

T [°]	$[Ag^+]_0 = 20$ mg/dm^3				$[Ag^+]_0 = 100$ mg/dm^3			
	O_2-free		O_2-saturated		O_2-free		O_2-saturated	
	n	*k'*	*n*	*k'*	*n*	*k'*	*n*	*k'*
15	5	1.34 ± 0.01	5	1.38 ± 0.02	5	1.34 ± 0.03	5	1.40 ± 0.04
25	30	1.83 ± 0.03	29	1.78 ± 0.03	7	1.81 ± 0.01	7	1.82 ± 0.05
35	6	2.33 ± 0.06	6	2.16 ± 0.03	6	2.55 ± 0.12	6	2.38 ± 0.07
55	6	3.93 ± 0.30	6	3.04 ± 0.05	7	3.63 ± 0.05	7	3.63 ± 0.33

The distribution histogram of the surface height calculated from the SEM image shown in *Fig. 1,a* shows a relatively narrow and intense peak. The wide range of surface heights existing in the positive region of the diagram corresponds closely with dendrites visible in SEM images. For the two temperatures above 15° (*Fig. 1,b* and *1,c*), the dendrites disappeared from the surface, but a new inhomogeneity appeared. This inhomogeneous surface was related now to anodic sites represented as a net of cracks. As a result of the disappearance of dendrites and the appearance of anodic sites on the reaction surface, the surface-height analysis performed from the SEM image for the experiment conducted at 35° (*Fig. 1,b*) showed a peak a little bit broader than the one shown in *Fig 1,a*. Further changes in the morphology of the Ag deposits obtained at 35 and 55° were clearly visible in the corresponding SEM images. The difference was closely connected with an increasing surface area of the anodic sites on the surface, especially at 55° (*Fig. 1,c*). This change was reflected in a significant broadening in the surface-height-distribution diagram.

To examine more closely the morphology of Ag deposits formed at various temperatures, higher-magnification SEM top-view images of the Ag-cemented Cu surface are shown in *Fig. 2* for the O_2-free solution containing 20 mg/dm^3 of Ag^+, together with the corresponding surface-height distributions. Here, the analyzed surface areas were *ca.* 20 μm^2. As can be seen from the SEM images, increasing temperature affected the morphology of the Ag deposits. At the lowest temperature (15°; *Fig. 2,a*), the deposit exhibited a tight well-adhered structure, with some separated large Ag crystals spread over the surface. These Ag crystals could grow due to the low rate of cementation (*Table 1*). As a result of this relatively tight deposit with separated crystals, the surface-height analysis of the SEM image showed a peak with a significant contribution of various heights in a range of positive values of the diagram heights.

Separated large Ag crystals did not appear at temperatures higher than 15° [27], where the rate of the cementation process is higher (*Figs. 2,b* and *2,c*). In the latter

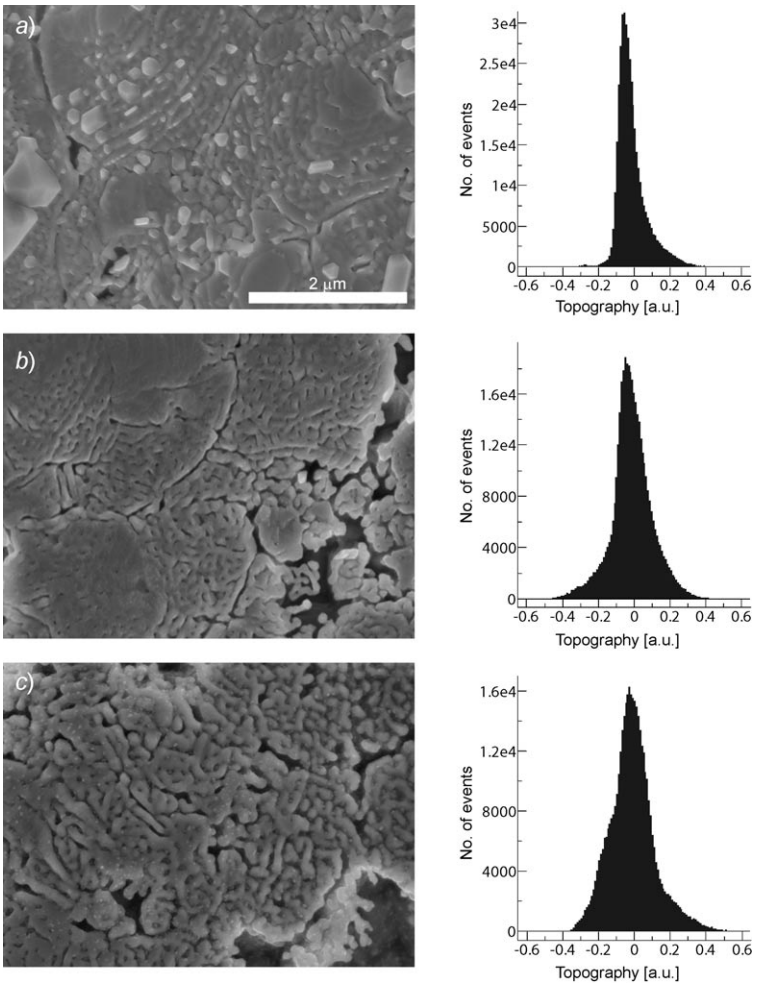

Fig. 2. *Images of* Fig. 1 *at higher resolution*. Analyzed surface area: *ca*. 20 µm^2.

case, the deposit becomes finer, but less tight, with visible tiny cracks. Consequently, broader peaks appeared in the corresponding surface-height-distribution histograms. Also, elevated temperatures gave rise to a number of mini-cracks between deposit grains, which led to some signal broadening in the height-distribution diagram.

The disappearance of separated Ag crystals and dendrites from the surface at process temperatures above 15° in O_2-free solutions is closely related to the decreasing percentage of cemented Ag found on the Cu surface after cementation. *Table 2* shows the average percentage of cemented Ag on the Cu surface as a function of the initial Ag^+ concentration (as determined by AAS) for both O_2-free and O_2-saturated solutions at initial Ag^+ concentrations of 20 or 100 mg/dm^3. As can be seen, the percentage of cemented Ag decreased rapidly with increasing temperature under O_2-free conditions at an Ag^+ concentration of 20 mg/dm^3. At 55°, only *ca*. 20% of the initial Ag^+ content

was found on the surface, which rationalizes the observed flattening effect in terms of surface roughness (*Fig. 2,b*).

Table 2. *Average Percentage* (*Θ*) *of Cemented Silver on Copper as a Function of Temperature, both under Oxygen-Free and Oxygen-Saturated Conditions.* The *Θ* values were determined by AAS. $[Ag^+]_0$ corresponds to the initial solution concentration of silver, *n* is the number of independent cementation experiments, and S_X (in %) is the standard deviation. For details, see *Experimental*.

T [°]	$[Ag^+]_0 = 20$ mg/dm^3						$[Ag^+]_0 = 100$ mg/dm^3					
	O_2-free			O_2-saturated			O_2-free			O_2-saturated		
	n	*Θ*	S_X	*n*	*Θ*	S_X	*n*	*Θ*	S_X	*n*	*Θ*	S_X
15	4	67.8	2.2	5	74.8	2.7	4	82.1	3.5	4	88.1	1.0
25	9	52.7	3.9	6	73.8	2.0	7	74.7	5.6	7	90.1	5.6
35	4	34.1	3.1	5	74.3	2.6	6	66.7	1.9	6	89.2	5.1
55	6	20.4	4.9	6	63.8	4.6	7	45.9	7.6	7	76.8	1.8

It is worth noting that the decrease of the percentage of cemented Ag is strictly related to the mechanism of the process conducted in O_2-free solution, and to the observation that the cemented Ag came off the rotating cylinder during the experiment. The contribution of the solution reaction presented in *Eqn. 1* to the overall cementation kinetics was estimated at *ca.* 30–40% at 25° [25][26]. With increasing temperature, this reaction should become more dominant due to the higher concentration of Cu^+ in solution [26]. Cu^+ Ions appear in solution as a result of the equilibrium between Cu^{2+} and Cu^0. The cemented Ag came off the cylinder due to the increasing surface area of the anodic sites during cementation, and due to the expansion of the anodic sites to parts on the surface that had previously been occupied by Ag deposits.

Next, we studied the cementation under O_2-saturated conditions at 20 mg/dm^3 initial Ag^+ solution concentration at temperatures of 15, 35, and 55°, respectively (*Fig. 3*). Similarly to the O_2-free reaction conducted at 15°, some dendrite germs were observed on the reaction surface under O_2-saturated conditions (*Fig. 3,a*). Again, at higher temperatures, they disappeared (*Figs. 3,b* and *3,c*). In contrast to the O_2-free experiment, separated Ag crystals of relatively large size were spread over the surface, even at 35°. This result is consistent with the percentage of cemented Ag observed for the O_2-saturated solution at 20 mg/dm^3 Ag^+ (*Table 2*). It can be seen that the percentage of cemented Ag remained almost constant in the temperature range of 15–35°. Obviously, the presence of O_2 significantly enhances the corrosion of Cu, and increasing temperature increases the rate of both processes: cementation (*Table 1*) and corrosion. As a result of enhanced Cu corrosion, the anodic sites are spread more uniformly over the reaction surface, forming a dense net of cracks (*Figs. 3,a* and *3,b*), or can develop their working surface area in the Cu material just under the deposited Ag, under formation of deep cavities (*Fig. 3,c*). Cavity formation has, actually, been reported before [26].

The expansion of the anodic sites at 55° resulted in more cemented Ag coming off the cylinder. As a consequence, lower percentage of cemented Ag were found on the surface (*Table 2*). For cementations performed under O_2 saturation at elevated temper-

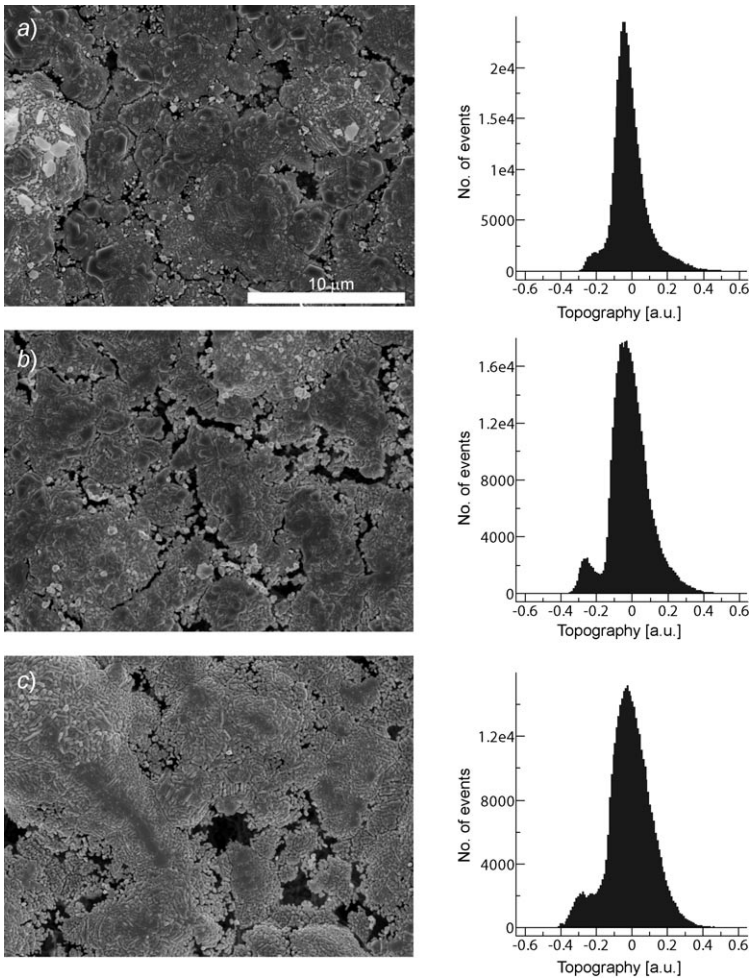

Fig. 3. *SEM Top-view images and surface-height-distribution diagrams for an O_2-saturated solution containing 20 mg/dm^3 Ag^+ at* a) *15°,* b) *35°, and* c) *55°.* Analyzed surface area: *ca.* 500 µm^2.

atures, two phenomena were observed in the SEM images: *1*) the disappearance of dendrites, and *2*) separated Ag crystals from the reaction surface at temperatures above 25 °C [27] and 35°, respectively. The second observation is related to the development of anodic sites. Both effects were observed in the SEM images presented in *Fig. 3*.

Increasing temperature modifies the roughness of Ag deposits due to increasing cementation rates. This effect is clearly exhibited in the surface-height-distribution diagrams. With increasing temperature, peak broadening occurred (*Figs. 3*, *b* and *3*, *c*). The presence of anodic sites on the surface is especially pronounced at negative depths. As expected due to enhanced Cu corrosion in O_2-saturated solutions, the surface-height distributions calculated from the SEM images were broader than those obtained by cementation of the corresponding O_2-free solutions. A comparison of the SEM images

of the Cu surfaces obtained at identical temperatures, but either under O_2-free (*Fig. 1*) or O_2-saturated conditions (*Fig. 3*) shows that the Ag deposit is flatter and smoother in the latter case. In aerobic solutions, the Ag deposit was found to be more granular. This difference can be rationalized in terms of the different percentages of cemented Ag on the surface, and differences in roughness of the deposits. From *Table 2*, it can be seen that the average percentage of cemented Ag is lower under O_2-free conditions than under O_2-saturated ones, except at 15°, where the values are similar.

Higher-magnification SEM images of the Cu surface with cemented Ag are presented in *Fig. 4* for O_2-saturated solutions (20 mg/dm^3 initial Ag^+). Closer examination of the reaction surface showed that the morphology of the Ag deposit was similar for the reactions performed at 15 and 35° (*Fig. 4,a* and *4,b*). The Ag deposits were found to cover the Cu surface with a uniform, tight layer, similar to the result observed previously for the experiment under O_2-free conditions at 15° (see *Fig. 2,a*). Moreover, the appearance of the Ag crystals formed at 15° in the presence or absence of O_2 was very similar. The broad peak in the surface-height-distribution diagram presented in *Fig. 4,a* exhibited a clearly inhomogeneous surface, with relatively large Ag crystals in the SEM image. When the temperature was increased to 35°, granular and finer crystals were formed in the O_2-saturated system, with a change in shape from an oval to an oblong shape. As expected, the temperature-dependent, increasing rate of cementation promoted formation of fine Ag crystals on the Cu surface. Simultaneously, anodic sites started to appear. As a consequence, a somewhat narrower peak was observed in the distribution diagram of the surface heights (*Fig. 4,b*).

A further increase in temperature to 55° resulted in loss of perfect tightness of the deposit, in combination with a further decrease of the dimensions of the deposited Ag crystals (*Fig. 4,c*). The corresponding peak broadening in the surface-height-distribution diagram indicates qualitatively a further expansion of the anodic-site area on the reaction surface. Finally, it is notable that the crystals grown at 35 and 55° from O_2-free solutions looked basically the same.

Figs. 5 and *6* show the SEM images of the sample surfaces (together with the corresponding surface-height distributions) at various temperatures for O_2-free and O_2-saturated solutions, respectively, but at higher initial Ag^+ concentration (100 mg/dm^3). For a given process temperature, the morphologies of the Ag deposits were not strongly affected by O_2, and the dendrites also looked very similarly. However, temperature had a great impact on morphology. At 15°, the dendrites formed huge 'lycopodium twigs-shape' crystallites on the surface (*Figs. 5,a* and *15,b*, and *Figs. 6,a* and *6,b*). These dendrites resulted in a very broad peak in the associated surface-height-distribution diagrams. At 15°, the reaction surface was very inhomogeneous, resulting in broad hight-distribution peaks under both aerobic and anaerobic conditions. When the temperature was increased to 25° (*Figs. 5,b* and *6,b*), the Ag deposits appeared denser and the 'lycopodium twigs' looked thicker. This means that the deposition proceeds mainly on the dendrites, which results in somewhat narrower peaks in the distribution diagrams (*Figs. 5,b* and *6,b*).

We also observed that the Ag crystallites formed from the O_2-saturated solutions were denser and occupied larger surface areas than those grown under O_2-free conditions (*Fig. 5,b vs. Fig. 6,b*). In the aerobic solution (*Fig. 6,b*), the dendrites covered almost the whole surface, and the peak in the distribution diagram was broader than

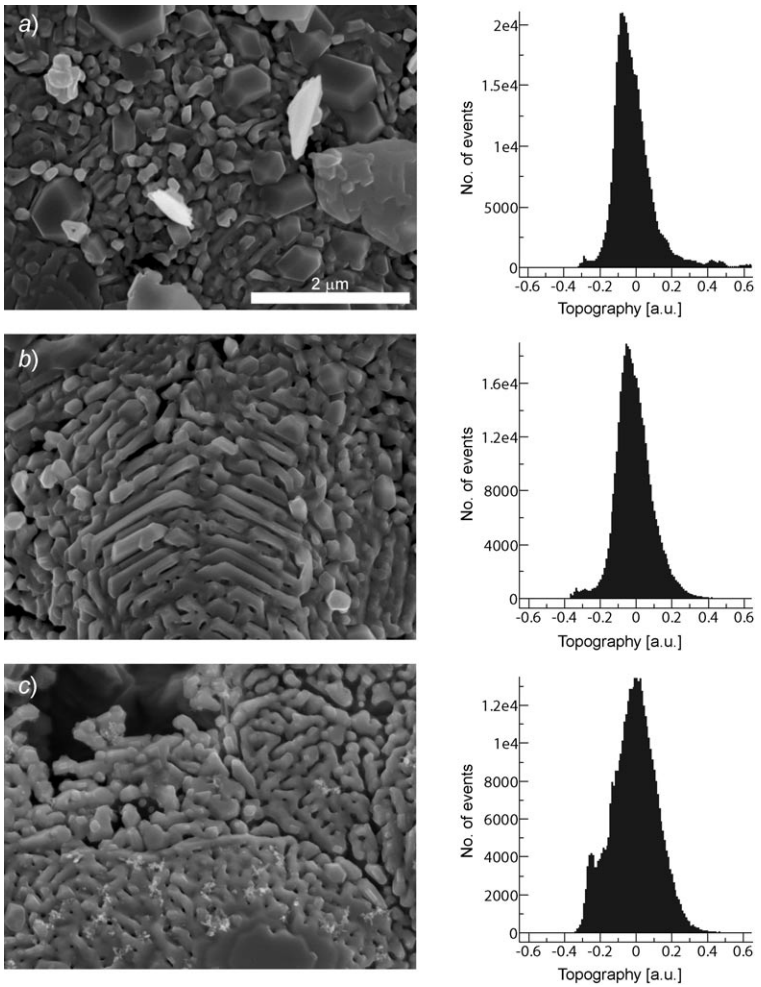

Fig. 4. *Images of* Fig. 3 *at higher resolution.* Analyzed surface area: *ca.* 20 µm^2.

that for the O_2-free experiment (*Fig. 5*,*b*). This can be attributed to the observation that, under O_2-saturated conditions, the average percentage of cemented Ag was higher than that under O_2-free conditions (*Table 2*).

When the temperature was increased to 35 or 55°, the Ag crystallites became more compact and denser, independent of the presence of O_2 (*Fig. 5*,*c* and *5*,*d*, *Fig. 6*,*c* and *6*,*d*). The surface areas occupied by the dendrites were smaller and, consequently, the peaks in the corresponding distribution diagrams were narrower and more intense. These results are consistent with the observed percentage of cemented Ag found on the Cu surface (*Table 2*). For the O_2-free solution containing 100 mg/dm^3 of Ag^+, the percentage of cemented Ag decreased rapidly with increasing temperature, mainly as a result of the progress of the competitive solution reaction (*Eqn. 1*), which consumed additional Ag^+ ions. In O_2-saturated solutions containing 100 mg/dm^3 of Ag^+, the per-

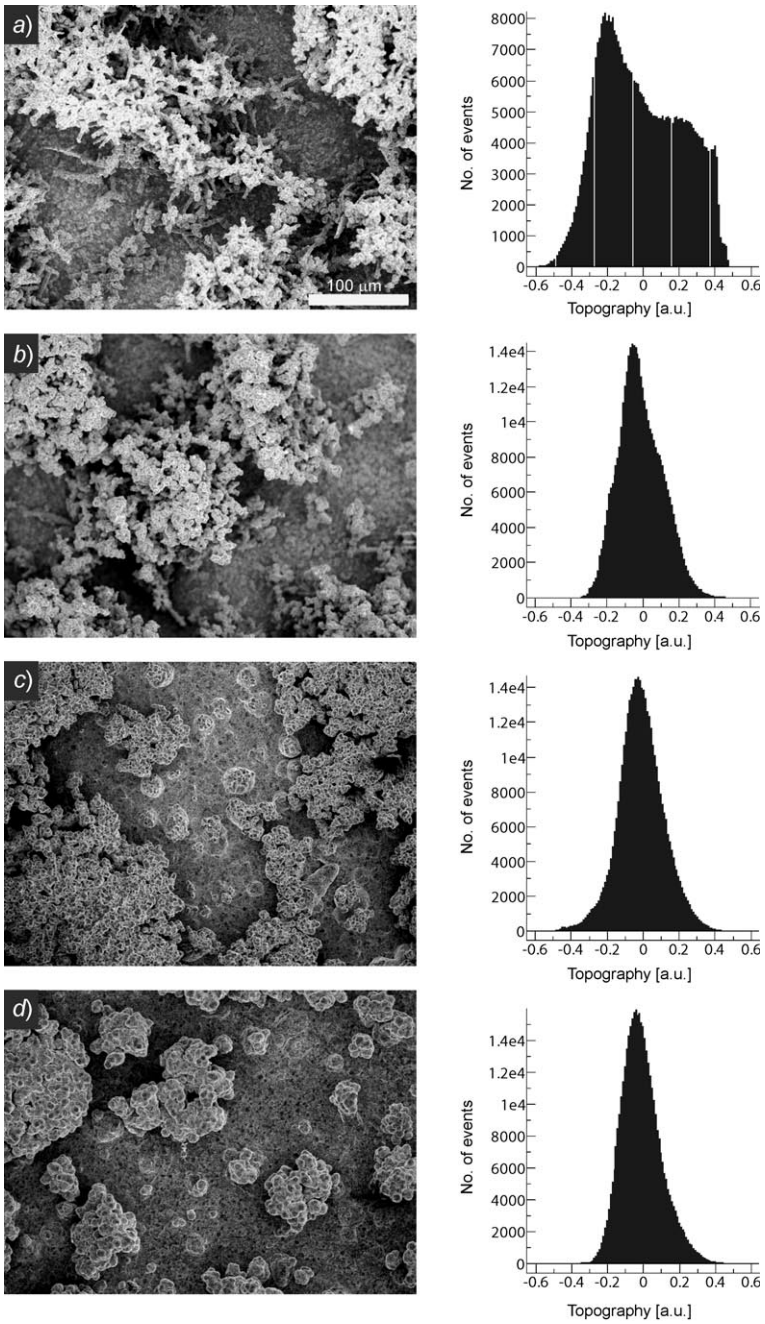

Fig. 5. *SEM Top-view images and surface-height-distribution diagrams for an O_2-free solution containing 100 mg/dm³ Ag^+ at* a) *15°,* b) *25°,* c) *35°, and d*) *55°.* Analyzed surface area: *ca.* 0.13 mm².

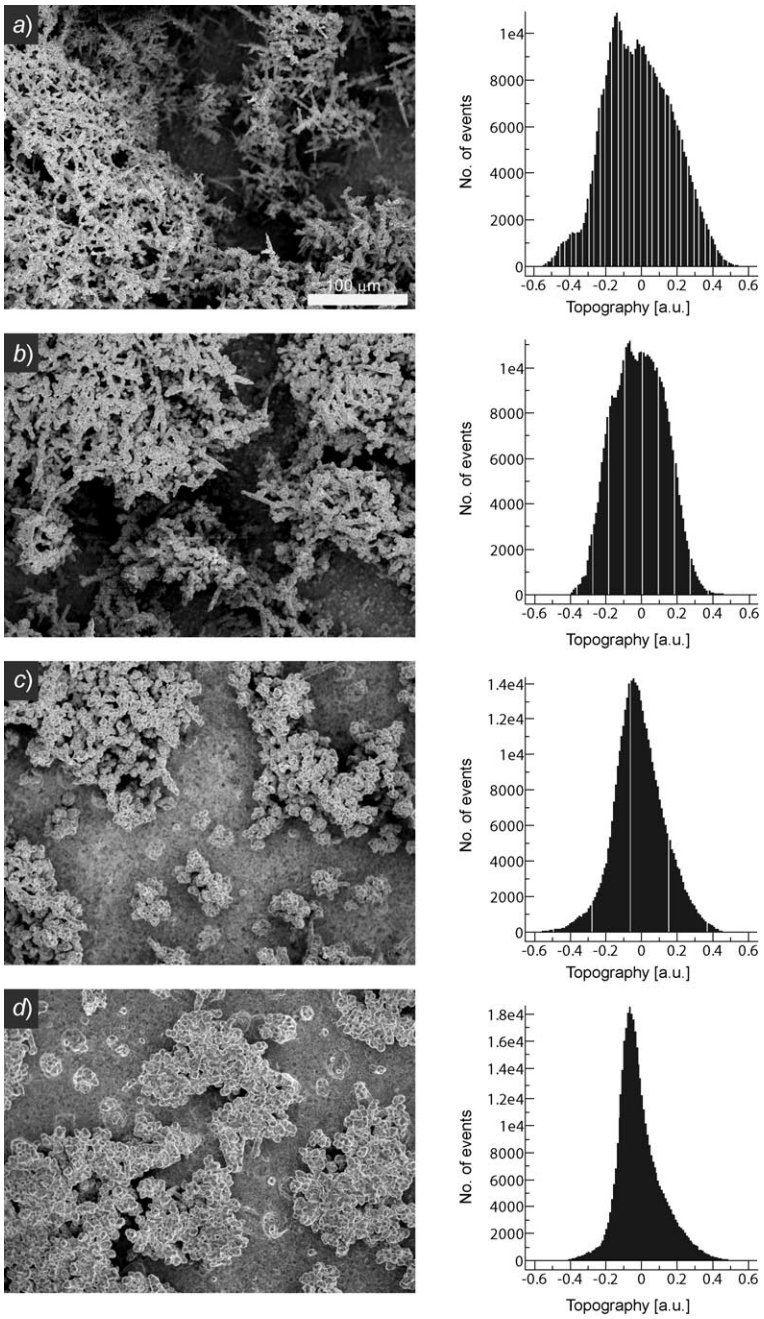

Fig. 6. *SEM Top-view images and surface-height-distribution diagrams for an O_2-saturated solution containing 100 mg/dm^3 Ag^+ at* a) *15°,* b) *25°,* c) *35°, and* d) *55°.* Analyzed surface area: *ca.* 0.13 mm^2.

centage of the cemented Ag remained constant between 15 and 35°. Finally, a decrease of *ca*. 10% in cemented Ag was observed when the temperature was raised to 55°. This was attributed to the observation that much of the cemented Ag came off the rotating cylinder. A similar decrease (10%) had been observed also in the experiment performed at lower Ag^+ concentration (see above).

To further illustrate the influence of temperature on the morphology of deposit during the cementation process conducted in the O_2-free and O_2-saturated solutions containing 100 mg/dm^3 Ag^+, higher-magnification SEM images are presented in *Fig. 7*. Detailed examination of the Ag crystallites formed at various temperatures showed that the presence of O_2 and temperatures below 35° did not significantly influence the morphology of the deposits. Relatively small morphological differences were found at a temperature of 35°. However, whereas under anaerobic conditions at 55° the Ag crystals were very fine and tiny, they became bigger and more uniform under aerobic conditions. The deposits formed huge porous crystallites with some vertical columns, independent of temperature and presence or absence of O_2. Also, the Cu surface was partially occupied by huge crystallites, but some parts of the surface were not covered by dendrites.

In *Fig. 8*, the higher-magnification SEM top-view image of a Cu surface with Ag deposits prepared at 35° under O_2-saturated conditions is shown. The image was taken from the part of the reaction surface that was not directly covered with dendrites. Here, the Ag crystals were distributed randomly over the surface without tightly covering the Cu surface. This part of the surface can, thus, play the role of the anodic site. The large dimension of the Cu crystal is partially visible at the bottom of the scattered, tiny Ag crystals. Similar observations of anodic sites were obtained at other temperatures under both O_2-free and O_2-saturated conditions (data not shown).

Conclusions. – When cementation is conducted in solutions containing 20 mg/dm^3 Ag^+ at 15°, germs of Ag dendrites are observed on the surface, independent of the presence or absence of O_2 in the system. The resulting deposits exhibit a tight, well-adhered structure, with some medium-sized Ag crystals spread over the surface. In the latter case, the surface-height distribution shows a peak with a significant contribution of various 'positive' heights (protruding elements). With increasing temperature, two independent phenomena are observed, which both affect the surface-height distribution. The first process is connected with the disappearance of dendrites from the surface, as indicated by peak narrowing in the distribution diagrams. The second is related to the formation and expansion of anodic sites on the surface, which results in peak broadening. Therefore, a contribution of various 'negative' surface heights (depressions) is observed. In O_2-saturated solutions, enhanced Cu corrosion leads to a denser net of anodic sites on the surface, and, as a result, the distribution histograms of the surface height exhibit broader peaks compared to those obtained in O_2-free experiments. The morphology of the Ag deposits is affected slightly by the presence of O_2 in the system. Under aerobic conditions, the deposits are granular up to a temperature of 35°. Morphological differences can be largely attributed to a different mechanism in the absence of O_2, leading to a different percentage of cemented Ag on the surface. The flattening effect of the surface roughness, observed mainly under O_2-free conditions, is connected with a competitive reaction in bulk solution (*Eqn. 1*) that consumes addi-

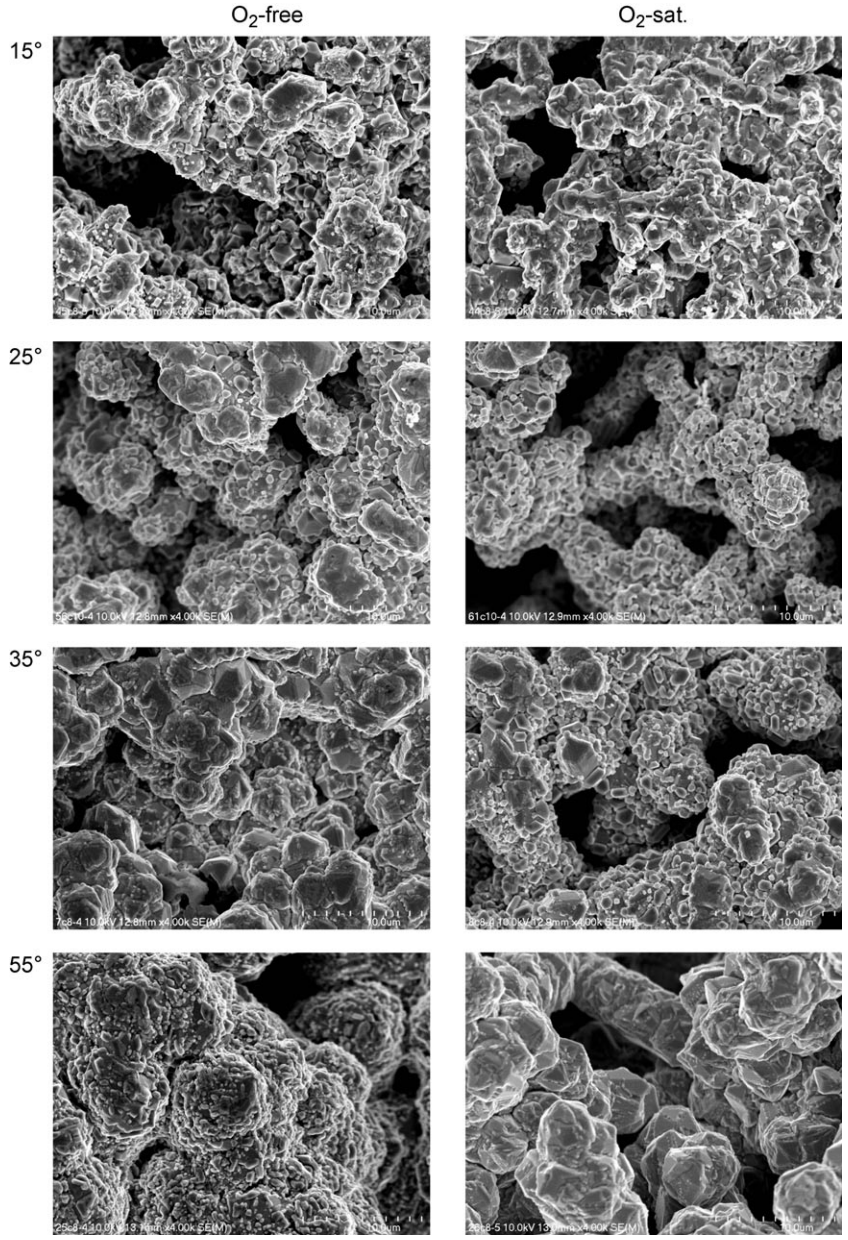

Fig. 7. *SEM Top-view images of cemented silver under O_2-free conditions* (left panel) *and O_2-saturated conditions* (right panel). Temperature (from top to bottom row): 15, 25, 35, and 55°, resp. Initial Ag^+ concentration: 100 mg/dm^3

tional Ag^+. As a result, lower amounts of cemented Ag are found on the surface after cementation. At a temperature of 55°, the cemented Ag readily comes off the rotating

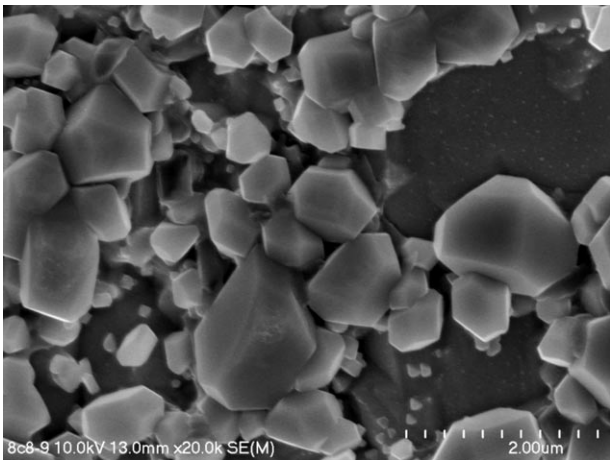

Fig. 8. *SEM Top-view image of the anodic site, with Ag crystals on the Cu surface grown from an O_2-saturated solution at 100 mg/dm^3 Ag^+*

cylinder as a result of the expansion of the anodic sites to parts on the surface that were previously occupied by Ag deposits.

The morphology of Ag deposits formed from solutions containing 100 mg/dm^3 of Ag^+ seems to be independent of the presence of O_2 in the system. Under O_2-saturated conditions, the resulting Ag dendrites are denser together and occupy a larger surface area than those formed under O_2-free conditions. This difference is also related to a different mechanism. With increasing temperature, Ag dendrites become more compact and denser, independent of the presence of O_2 in solution. The changes in the morphology of the Ag deposits are clearly reflected in the corresponding surface-height-distribution diagrams.

In general, one can say that both morphology and roughness of Ag deposits formed on Cu by cementation vary significantly with temperature, as readily reflected in their surface-height distribution. Therefore, SEM in combination with surface analysis provides useful information about the evolution of anodic and cathodic sites during cementation, and the results can be rationalized in terms of mechanism and process kinetics.

We kindly acknowledge the Laboratory of Field Emission Scanning Electron Microscopy and Microanalysis at the Institute of Geological Sciences, Jagiellonian University (Poland), where SEM imaging has been performed.

REFERENCES

[1] R. Gana, M. Figueroa, L. Kattan, D. Grandoso, M. A. Esteso, *J. Appl. Electrochem.* **1999**, *29*, 1475.
[2] D. Stanojević, B. Nikolić, M. Todorović, *Hydrometallurgy* **2000**, *54,* 151.
[3] I. Bojanowska, *Pol. J. Environ. Stud.* **2002**, *11,* 225.
[4] F. A. López, M. I. Martín, C. Pérez, A. López-Delgado, F. J. Alguacil, *Water Res.* **2003**, *37*, 3883.
[5] M.-S. Lee, J.-G. Ahn, J.-W. Ahn, *Hydrometallurgy* **2003**, *70*, 23.
[6] M. El-Batouti, J. Colloid Interface Sci. **2005**, 283, 123.
[7] K. Stefanowicz, M. Osińska, S. Napieralska-Zagozda, *Hydrometallurgy* **1997**, *47*, 69.

[8] K. Stole-Hansen, D. A. Wregget, D. Gowanlock, P. E. Thwaites, *Comput. Chem. Eng.* **1997**, *21*, S1099.
[9] A. M. Sullivan, P. A. Kohl, *J. Electrochem. Soc.* **1997**, *144*, 1686.
[10] I. B. Murashova, G. V. Ostarkova, N. G. Burkhanova, *Russ. J. Electrochem.* **2002**, *38*, 247.
[11] T. M. Dreher, A. Nelson, G. P. Demopoulos, D. Filippou, *Hydrometallurgy* **2001**, *60*, 105.
[12] B. B. Boyanov, V. V. Konareva, N. K. Kolev, *Hydrometallurgy* **2004**, *73*, 163.
[13] J. Näsi, *Hydrometallurgy* **2004**, *73*, 123.
[14] J. Y. Choi, D. S. Kim, *J. Hazard. Mater., B* **2003**, *99*, 147.
[15] Y. Ku, M.-H. Wu, Y.-S. Shen, *Waste Manage.* **2002**, *22*, 721.
[16] S. A. Nosier, *Chem. Biochem. Eng. Q.* **2003**, *17*, 219.
[17] A. Dib, L. Makhloufi, *Chem. Eng. Process.* **2004**, *43*, 1265.
[18] A. A. Mubarak, A. H. El-Shazly, A. H. Konsowa, *Desalination* **2004**, *167*, 127.
[19] M. El-Batouti, *Anti-Corros. Meth. Mater.* **2005**, *52*, 42.
[20] G. V. Ostarkova, I. B. Murashova, N. O. Esina, A. A. Pankratov, *Powder Metall. Metal Ceram.* **1999**, *38*, 344.
[21] Z.-Y. Jiang, Z.-X. Xie, S.-H. Zhang, S.-Y. Xie, R.-B. Huang, L.-S. Zheng, *Chem. Phys. Lett.* **2003**, *374*, 645.
[22] P. Ernst, A. Earnshaw, I. P. Wadsworth, G. W. Marshall, *Corros. Sci.* **1999**, *39*, 1329.
[23] J.-H. Shin, K.-W. Kim, H.-J. Ahn, *J. Power Sources* **2000**, *89*, 46.
[24] M. H. Pournaghi-Azar, Biuck Habibi-A, *J. Electroanal. Chem.* **2005**, *580*, 23.
[25] G. D. Sulka, M. Jaskuła, *Hydrometallurgy* **2002**, *64*, 13.
[26] G. D. Sulka, M. Jaskuła, *Hydrometallurgy* **2004**, *72*, 93.
[27] G. D. Sulka, M. Jaskuła, *Hydrometallurgy* **2005**, *77*, 131.
[28] WSxM 3.0, Nanotec Electronica SL, Spain (http://www.nanotec.es).

Received October 27, 2005